Molecular Therapy
Methods & Clinical Development
Original Article

Bezafibrate Enhances AAV Vector-Mediated Genome Editing in Glycogen Storage Disease Type Ia

Hye-Ri Kang,[1] Lauren Waskowicz,[1] Andrea M. Seifts,[1] Dustin J. Landau,[1] Sarah P. Young,[1] and Dwight D. Koeberl[1]

[1]Division of Medical Genetics, Department of Pediatrics, Duke University Medical Center, Durham, NC 27710, USA

Glycogen storage disease type Ia (GSD Ia) is a rare inherited disease caused by mutations in the glucose-6-phosphatase (G6Pase) catalytic subunit gene (*G6PC*). Absence of G6Pase causes life-threatening hypoglycemia and long-term complications because of the accumulations of metabolic intermediates. Bezafibrate, a pan-peroxisome proliferator-activated receptor (PPAR) agonist, was administered in the context of genome editing with a zinc-finger nuclease-containing vector (AAV-ZFN) and a G6Pase donor vector (AAV-RoG6P). Bezafibrate treatment increased survival and decreased liver size (liver/body mass, $p < 0.05$) in combination with genome editing. Blood glucose has higher ($p < 0.05$) after 4 h of fasting, and liver glycogen accumulation ($p < 0.05$) was lower in association with higher G6Pase activity ($p < 0.05$). Furthermore, bezafibrate-treated mice had increased numbers of *G6PC* transgenes ($p < 0.05$) and higher ZFN activity ($p < 0.01$) in the liver compared with controls. PPAR-α expression was increased and PPAR-γ expression was decreased in bezafibrate-treated mice. Therefore, bezafibrate improved hepatocellular abnormalities and increased the transduction efficiency of AAV vector-mediated genome editing in liver, whereas higher expression of G6Pase corrected molecular signaling in GSD Ia. Taken together, bezafibrate shows promise as a drug for increasing AAV vector-mediated genome editing.

INTRODUCTION

Glycogen storage disease type Ia (GSD Ia), also known as von Gierke's disease, is an inherited metabolic disease caused by mutations in the *G6PC* gene encoding glucose-6-phosphatase (G6Pase), an endoplasmic reticulum (ER)-resident enzyme that is mainly expressed in liver and kidney. G6Pase converts glucose-6-phosphate (G6P) to glucose and phosphate (P_i), which is the final step in both glycogenolysis and gluconeogenesis.[1] Therefore, G6Pase deficiency causes an excessive accumulation of G6P, resulting in accumulations of glycogen and triglycerides in the liver. GSD Ia is characterized by life-threatening hypoglycemia, growth retardation, hepatomegaly, nephromegaly, hyperlipidemia, hyperuricemia, and lactic acidemia.[1] Current dietary therapy can manage hypoglycemia and has extended the life expectancy of patients, but fails to prevent long-term complications including chronic kidney disease, nephrolithiasis, gout, pulmonary hypertension, hepatocellular adenomas (HCAs), and a high risk for hepatocellular carcinoma (HCC).[2–6] Therefore, new therapies are needed for GSD Ia.

Recombinant adeno-associated virus vector-mediated gene therapy has proved to be efficacious in disease models.[7] However, adeno-associated virus (AAV) vector genomes are gradually lost from dividing cells, and readministration of the vector cross-packaged with a new AAV serotype is required to maintain transgene expression and to avoid anti-AAV antibody formation in the liver.[8–11] AAV vector administration to young mice achieved a high level of liver transduction, followed by a gradual decline in vector genomes over the ensuing months.[12–15] For example, an AAV2/8 vector decreased from >2 copies per liver cell at 1 month of age to 0.3 copy at 7 months of age in G6Pase-knockout (KO) mice.[12] Similarly, an AAV2/8 vector was administered to a GSD Ia puppy at 1 day of age and prevented hypoglycemia for 3 h at 1 month of age; however, by 2 months of age the dog became hypoglycemic after 1 h of fasting.[11] Genome editing to achieve integration of a *G6PC* transgene encoding G6Pase, facilitated by a zinc-finger nuclease (ZFN) that cleaves the murine *ROSA26* safe harbor locus, improved vector persistency and efficacy in the *G6pc*$^{-/-}$ mouse model.[15] However, the hepatocellular abnormalities of GSD Ia, including increased apoptosis, inflammation, and impaired autophagy, represent a challenge to liver-directed gene therapy or genome editing in GSD Ia.[16,17]

Autophagy is an adaptive process that occurs in response to different forms of stress, including nutrient deprivation, growth factor depletion, infection, and hypoxia.[18] Autophagy activates the lysosomal degradation of glycogen to glucose and lysosomal proteolysis that provides amino acids for gluconeogenesis during fasting.[17,19] In addition, pharmacological inducers of autophagy stimulate AAV vector transduction efficiency.[20] Therefore, inducing autophagy could provide a strategy to treat hepatic abnormalities, in addition to increasing the efficiency of AAV transduction in the GSD Ia liver.

Received 30 January 2019; accepted 6 February 2019;
https://doi.org/10.1016/j.omtm.2019.02.002.

Correspondence: Dwight D. Koeberl, Division of Medical Genetics, Department of Pediatrics, Duke University Medical Center, Box 103856, Durham, NC 27710, USA.
E-mail: dwight.koeberl@duke.edu

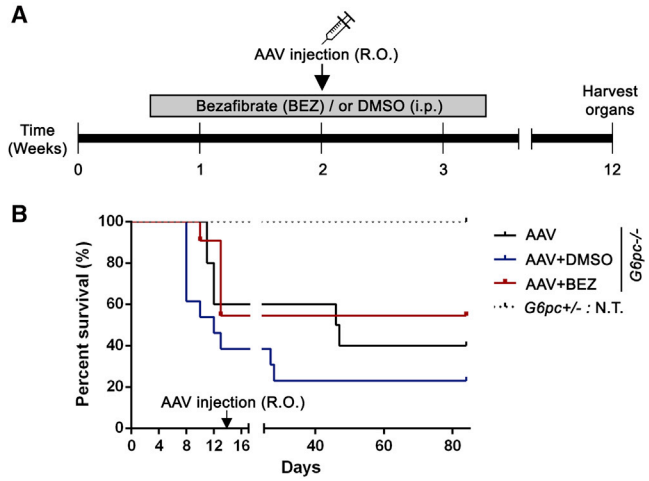

Figure 1. Survival Curve of Mice on Each Group

(A) Mice were treated with bezafibrate (12.5 mg/kg) from 5 days of age for 3 weeks. AAV was injected at 14 days of age. At 3 months of age, organs were harvested. (B) Bezafibrate treatment increased survival rate compared with the DMSO-treated group (p = 0.047, using Gehan-Breslow-Wilcoxon test). Survival was plotted as a Kaplan-Meier curve.

Bezafibrate is a fibric acid derivative that has serum triglyceride-lowering and high-density lipoprotein cholesterol (HDL-C)-elevating actions.[21] Bezafibrate functions as a pan-agonist of peroxisome proliferator-activated receptors (PPARs), including PPAR-α, -γ, and -β/δ, which enhances the expression of genes involved in lipid homeostasis, energy metabolism, antioxidant defenses, and mitochondrial biogenesis.[21,22] Increased expression of PPAR-γ has been demonstrated in the neonatal *G6pc*$^{-/-}$ mouse model, whereas PPAR-α expression was decreased.[23] Downregulation of sirtuin 1 (SIRT1) was associated with defective autophagy in adult, liver-specific *G6pc*$^{-/-}$ mice with GSD Ia.[23] Importantly, upregulating PPAR-α improved hepatic autophagy and fatty acid β-oxidation,[24,25] which suggested that a PPAR agonist might have beneficial effects in GSD Ia.

We previously reported that impaired autophagy is induced by rapamycin treatment, a mechanistic target of rapamycin (mTOR) inhibitor, which leads to significant reduction of hepatic glycogen and triglycerides by inducing autophagy in *G6pc*$^{-/-}$ mice with the GSD Ia model.[26] Similarly, bezafibrate stimulated fatty acid oxidation and induced autophagy, and decreased hepatic glycogen and triglycerides by inducing autophagy in *G6pc*$^{-/-}$ mice.[27] Given its beneficial effects in the GSD Ia liver, we evaluated the effect of bezafibrate in combination with AAV vector-mediated genome editing in *G6pc*$^{-/-}$ mice.

RESULTS

Bezafibrate had the beneficial effects of reducing accumulated hepatic triglycerides and glycogen by increasing autophagy and fatty acid oxidation, and decreasing fatty acid synthase expression in *G6pc*$^{-/-}$ mice.[27] However, bezafibrate treatment itself failed to reverse hypoglycemia or to prolong the survival of neonatal *G6pc*$^{-/-}$ mice. We hypothesized that the efficiency of AAV vector-mediated genome editing would be enhanced by treatment with bezafibrate to reverse the hepatocellular abnormalities associated with GSD Ia. Therefore, we evaluated the effect of administering bezafibrate (or vehicle) during genome editing, starting at 5 days of age for 3 weeks. Genome-editing vectors, AAV2/9-RoG6P and AAV2/9-ZFN,[15] were administrated into all *G6pc*$^{-/-}$ mouse groups at 14 ± 1 days of age. *G6pc*$^{+/-}$ mice were not treated with either AAV vectors or drugs. Mice were euthanized for tissue analysis at 3 months of age (Figure 1A and Table S1). AAV vector-injected *G6pc*$^{-/-}$ mice survived for up to 12 weeks, whereas historically untreated *G6pc*$^{-/-}$ mice survived only 2 weeks despite the administration of daily dextrose injections to treat hypoglycemia.[28] Moreover, bezafibrate-treated mice uniformly survived following vector administration at 2 weeks of age, in contrast with DMSO (vehicle)-treated mice, demonstrating enhanced survival in comparison with vehicle-treated *G6pc*$^{-/-}$ mice ($p < 0.05$) (Figure 1B).

G6pc$^{-/-}$ mice develop hepatomegaly and hepatosteatosis because of the accumulation of G6P, which drives the accumulation of glycogen and triglycerides.[29] Bezafibrate-treated mice had decreased liver mass, in comparison with vehicle-treated or AAV vector-only mice (Figure 2A). Similarly, hepatic glycogen was significantly decreased in bezafibrate-treated mice, in comparison with AAV vector-only mice (Figure 2B). Hepatic triglycerides were normalized in all groups, demonstrating that vector administration alone reversed hepatosteatosis (Figure 2C). The glucose tolerance test (GTT) revealed abnormal glucose metabolism in all groups of *G6pc*$^{-/-}$ mice (Figure 2D). However, bezafibrate treatment increased blood glucose after 4 h of fasting (151 ± 9.7 mg/dL), in comparison with vehicle (112 ± 12.4 mg/dL) or vector alone (98 ± 4.0 mg/dL) (Figure 2E).

We evaluated the effect of bezafibrate upon kidney involvement in *G6pc*$^{-/-}$ mice, which revealed enlarged kidneys, in comparison with *G6pc*$^{+/-}$ mice (Figure S1A). AAV vector-mediated gene therapy has not completely reversed the renal involvement of GSD Ia.[30] Glycogen and G6Pase activity were unchanged by bezafibrate treatment (Figures S1B and S1C), and vector genomes were very low in the kidney (Figure S1D). Thus, bezafibrate with AAV vector administration did not correct renal involvement in *G6pc*$^{-/-}$ mice.

Biochemical abnormalities include lactic acidemia in GSD Ia patients and elevated urinary lactate in *G6pc*$^{-/-}$ mice.[12,31] G6Pase deficiency results in the diversion of G6P into glycolysis and the production of pyruvate, as well as diversion into the pentose phosphate pathway. The production of excess pyruvate leads to the production of excess lactate, resulting in lactic acidemia and lactic aciduria. To evaluate the effect of bezafibrate alone, we administered bezafibrate or DMSO (vehicle) for 5 days and collected urine at the age of 10 days. Young *G6pc*$^{-/-}$ non-treated (N.T.) mice had increased urinary pyruvate and lactate, in comparison with unaffected mice (Figures 2F and 2G). Urinary lactate was decreased following bezafibrate administration in 10-day-old *G6pc*$^{-/-}$ mice, in comparison with N.T. and DMSO controls (Figures 2F and 2G, left four bars). Urinary

pyruvate and lactate concentrations were similar in all groups of adult *G6pc*$^{-/-}$ mice following vector administration at 3 months, similar to those of unaffected mice (Figures 2F and 2G, right four bars). Thus, bezafibrate treatment decreased urinary lactate accumulations in young *G6pc*$^{-/-}$ mice, and AAV vector administration was sufficient to correct urinary lactate accumulations in adult *G6pc*$^{-/-}$ mice.

Transgene expression in liver was analyzed to better explain the correction of hepatic abnormalities by bezafibrate treatment in *G6pc*$^{-/-}$ mice. Bezafibrate treatment increased G6Pase activity in association with a high level of *G6PC* mRNA expression derived from the AAV2/9-RoG6P donor vector (Figures 3A and 3B). Histochemical staining of G6Pase was undetectable in untreated *G6pc*$^{-/-}$ mice, in contrast with *G6pc*$^{+/-}$ mice that showed uniform staining throughout the liver (Figure 3C). Bezafibrate treatment markedly increased the number of G6Pase-positive cells in vector-treated mice, in comparison with the DMSO (vehicle) and AAV-only mice, which revealed similar numbers of G6Pase-positive cells (Figures 3C and 3D). Next, to determine whether bezafibrate treatment had an effect on the persistence of the AAV vectors, we quantified AAV vector genomes in liver. Higher numbers of AAV-RoG6P and AAV-ZFN vector genomes were present in bezafibrate-treated mice, in comparison with AAV-only mice (Figures 4A and 4B). The AAV-RoG6P and AAV-ZFN vectors were designed to integrate the human *G6PC* transgene into the *Rosa26* target site.[15] To quantify ZFN activity at the target site, we performed Surveyor nuclease assay with genomic DNA in the liver. The average allele modification rate (Indels %) in bezafibrate-treated mice (5.5% ± 0.76%) was significantly higher than in either the DMSO (vehicle) (1.7% ± 0.24%) or AAV-only groups (2.0% ± 0.24%) (Figures 4C and 4D). To confirm transgene integration in *Rosa26*, we performed nested PCR, which detected *G6PC* transgene integration in all AAV-treated mice (Figure 4E). Thus, bezafibrate treatment enhanced transgene persistence, which led to increased AAV2/9-RoG6P-derived G6Pase expression in the liver and improved biochemical correction.

Next, molecular signaling was investigated to assess the synergistic bezafibrate effect in combination with AAV vector-mediated genome editing. Liver-specific G6Pase deficiency results in decreased expression of PPAR-α, a key transcription factor of hepatic lipid metabolism, and increased expression of PPAR-γ, a master regulator of adipogenesis.[23] The expression of PPAR-α and PPAR-γ were not completely normalized to the level observed in *G6pc*$^{+/-}$ mice following AAV vector administration (Figures 5A–5C). However, bezafibrate treatment significantly increased PPAR-α and suppressed PPAR-γ, in comparison with the DMSO (vehicle) and AAV-only groups (Figures 5A–5C). Impaired PPAR signaling contributes to the downregulation of *SIRT1* expression, which leads to autophagy impairment in adult liver-specific *G6pc*$^{-/-}$ mice.[23] Furthermore, impaired autophagy was attributed to hepatosteatosis in neonatal complete *G6pc*$^{-/-}$ mice, which was reversed by administration of an AAV vector encoding G6Pase.[26] Consistent with the latter observation, AAV vector administration alone was sufficient to normalize autophagic flux, as assessed by LC3B-II expression and SIRT1 expression in *G6pc*$^{-/-}$ mice, and bezafibrate administration had no additional effects (Figures S2A–2C).

DISCUSSION

These experiments demonstrated the beneficial effects of bezafibrate treatment prior to the administration of AAV vectors to accomplish genome editing in GSD Ia. Bezafibrate activates fatty acid oxidation and induces autophagy in the GSD Ia liver,[27] and bezafibrate treatment with genome editing enhanced the benefits compared with each treatment alone in the current study. Liver G6Pase activity was increased and glycogen content was decreased to a greater extent from bezafibrate treatment following the administration of AAV vector-mediated genome editing, which correlated with improved prevention of hypoglycemia during fasting. The activity of the ZFN was enhanced by bezafibrate treatment, which correlated with greater retention of the G6PC transgene. Abnormalities of signaling were normalized by bezafibrate treatment with genome editing, including the expression of PPAR-α and PPAR-γ. Thus, pretreatment with bezafibrate normalized the GSD Ia liver and enhanced the effects of genome editing.

GSD Ia causes hepatosteatosis that suppresses autophagy.[23,26] Treatment with autophagy-inducing drugs decreased the accumulation of glycogen and triglycerides in the liver of mice with GSD Ia without correcting hypoglycemia or prolonging survival.[26] We hypothesized that inducing autophagy with a small-molecule drug such as bezafibrate might improve the efficiency of genome editing and increase the long-term correction of G6Pase deficiency in the GSD Ia liver. The cumulative results of this study support that hypothesis and further validate the general hypothesis that combination therapy will enhance the effects of gene therapy.[32–34]

Although genome editing has advantages over gene replacement therapy with regard to the persistence of the therapeutic transgene in the liver, genome editing has not corrected all cells in the liver.[15,35] The efficiency of genome editing has been low in GSD Ia, possibly related to the associated hepatocellular abnormalities that include increased apoptosis[16] that drives the well-demonstrated loss of AAV vector genomes.[12,28,36,37] Here we demonstrated that treatment with bezafibrate prior to the administration of AAV vectors achieved greater genome editing and stabilized the *G6PC* transgene in the liver. These effects might also derive from the induction of autophagy, which has been shown to increase the transduction of hepatocytes with AAV vectors.[20]

This study did not achieve the correction of renal involvement from GSD Ia, similarly to previous studies of AAV vector-mediated gene delivery.[12,28,36] Although recombinant AAV9 vectors such as those used here might have improved efficiency of transduction in the kidney,[30] genome editing was impacted by the choice of a liver-specific promoter for expression of the ZFN.[15] Thus, future genome editing in GSD Ia might be enhanced by selecting a serotype and promoter to achieve nuclease expression in the kidney as well as liver.

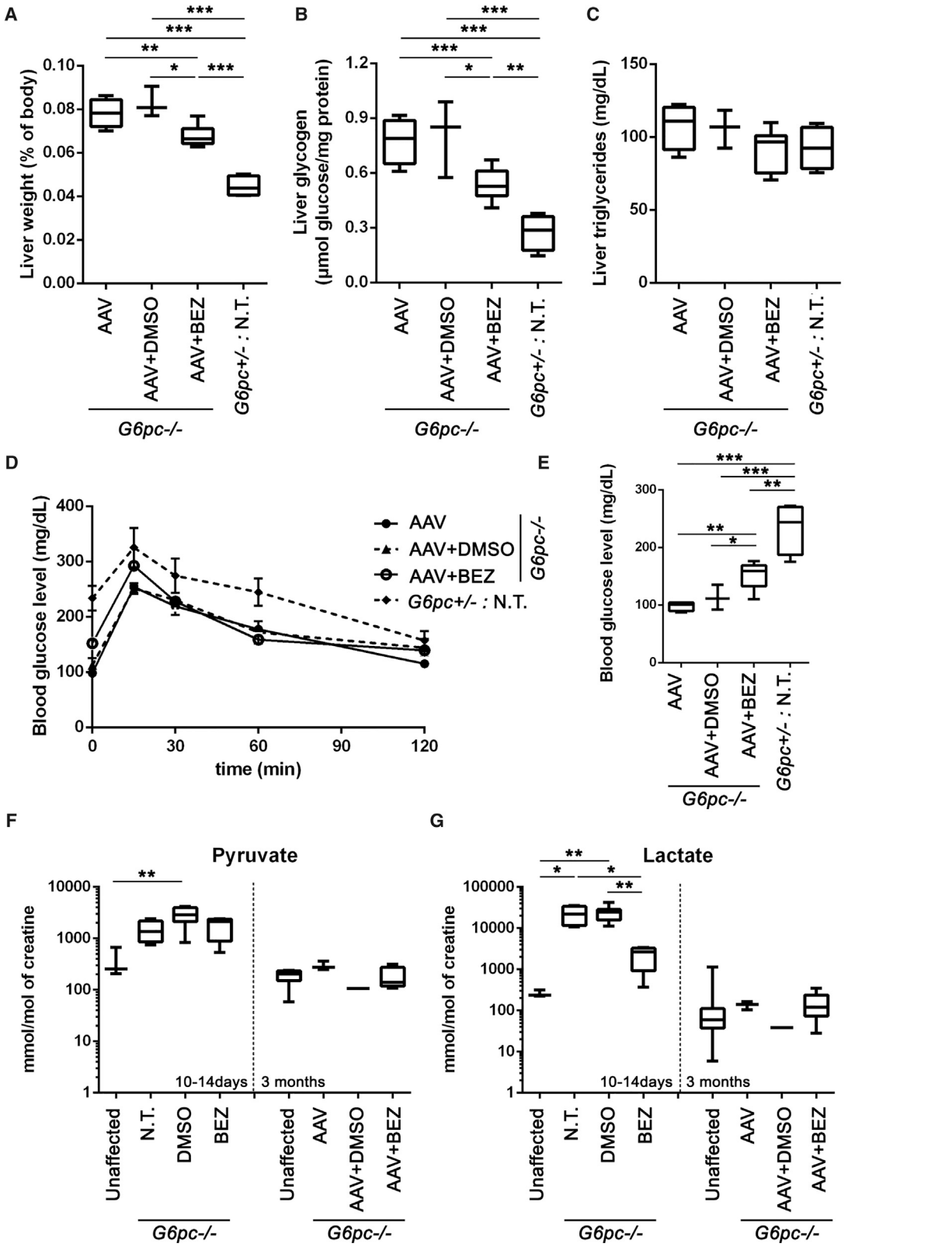

(legend on next page)

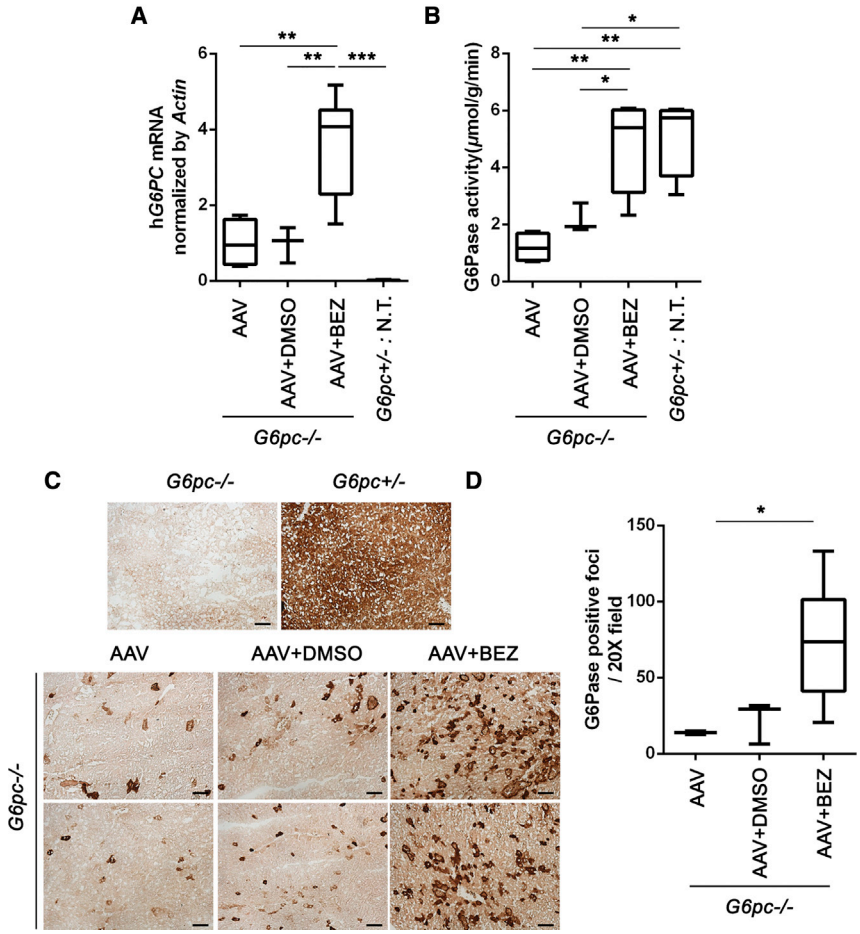

Figure 3. *G6PC* Expression in the Liver

(A) AAV-derived *G6PC* mRNA levels were measured, and relative expression level of genes was determined by normalization relative to that of *Actin*. Bezafibrate-treated mice had higher expression compared with other groups. (B) G6Pase activity in the liver was significantly higher *G6PC* in bezafibrate-treated mice. (C) Representative G6Pase staining sections in the liver of each group. Bezafibrate-treated mice had significant enhancement in G6Pase-positive cell numbers. $G6pc^{-/-}$ mice are 14 days of age, and $G6pc^{+/-}$ mice are 3 months of age. Dark brown spots indicate G6Pase-positive cells. (D) G6Pase-positive cells were counted and analyzed with ImageJ. Scale bars indicate 200 μm. Group sizes are: AAV, n = 4 (D; n = 3); AAV+DMSO, n = 3; AAV+BEZ, n = 6; unaffected, n = 4. Mean ± SE is shown. *p < 0.05, **p < 0.01, ***p < 0.001, ****p < 0.0001 from ANOVA. BEZ, bezafibrate.

In summary, bezafibrate improved the hepatic environment and increased the transduction efficiency of AAV vectors to achieve more effective genome editing in the GSD Ia liver, whereas higher *G6PC* transgene expression corrected molecular signaling. Taken together, bezafibrate shows promise not only as a treatment in GSD Ia, but also as a drug for increasing AAV vector transduction and genome-editing efficiency.

MATERIALS AND METHODS

Study Approval

All animals received human care, and animal studies were approved by Duke University Institutional Animal Care and Use Committee (IACUC) under the protocol A038-17-02.

Preparation of AAV Vectors

The AAV vector plasmids, AAV2/9-RoG6P and AAV2/9-ZFN, were previously described.[15] In brief, AAV2/9-RoG6P contained the human G6Pase, which was flanked by sequences from exon 1 of the mouse ROSA26 locus. AAV2/9-ZFN contained the transgene for the two subunits of the ROSA26-targeting "R4L6 eZFN." For the production of AAV vectors by transfection, HEK293 cells were transfected using calcium phosphate transfection methods. After 48 h, cells were resuspended in lysis buffer (50 mM Tris, 150 mM NaCl [pH 8.5]). Cells were then lysed by three freeze-thaw cycles and incubated with Benzonase nuclease (E1014; Sigma) at 37°C for 1 h. After pelleting cell debris for 20 min at 3,000 × *g*, the supernatant was used for further purification. Sucrose solution (40%) was used to pellet the crude viral particles by centrifugation at 28,000 × *g* for 20 h at 4°C. The pellet was resuspended vigorously with 1× Hank's balanced salt solution (HBSS), mixed with the same volume of 2× medium CsCl (final concentration is 1.37 g/mL [pH 8.0]), and transferred to an ultracentrifugation tube (06752; Thermo Scientific). The vector solution was layered over 1 mL of heavy CsCl (1.50 g/mL [pH 8.0]) and centrifuged at 40,000 × *g* for 20 h at 4°C. The band of viral particles was collected and transferred to a second two-tier CsCl gradient. Viral fractions were pooled and applied to three rounds of dialysis against 2 L of 5% sorbitol solution, using Slide-A-Lyzer MWCO (molecular weight cutoff) 10,000 dialysis

Figure 2. Biochemical Correction following Treatment

(A) Liver weight was measured and normalized by each body mass. (B) Hepatic glycogen accumulation was reduced in bezafibrate-treated mice, in comparison with either DMSO or N.T. mice. (C) Hepatic triglycerides revealed no significant differences between groups. (D) Glucose tolerance test (GTT) for all mice. Mice were fasted for 4 h and then injected with glucose (10 μL/g, intraperitoneal). Blood glucose concentrations were determined with a glucometer using blood samples from cut tail tips at the indicated time points. (E) After 4 h fasting, bezafibrate-treated mice maintained higher blood glucose compared with DMSO and N.T. mice. Group sizes are: AAV, n = 4; AAV+DMSO, n = 3; AAV+BEZ, n = 6; unaffected, n = 4. Urinary pyruvate (F) and lactate (G). Group sizes for young mice (10–14 days) are: unaffected (treated with DMSO), n = 3; N.T., n = 5; DMSO, n = 10; BEZ, n = 4. Group sizes for adult mice (3 months) are: unaffected (N.T.), n = 5; AAV, n = 3; AAV+DMSO, n = 1; AAV+BEZ, n = 5. Mean ± SE is shown. *p < 0.05, **p < 0.01, ***p < 0.001, ****p < 0.0001 from ANOVA. BEZ, bezafibrate.

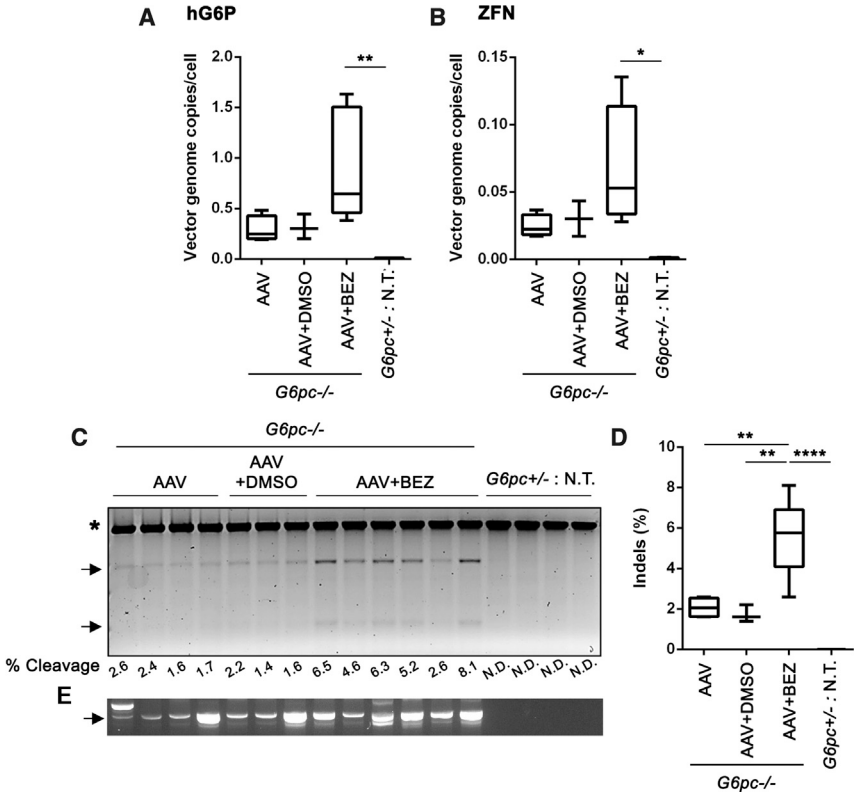

Figure 4. Transduction Efficiency and Nuclease Activity in the Liver

(A and B) AAV2/9-RoG6P (A) and AAV2/9-ZFN (B) were quantified in liver DNA. (C) Surveyor nuclease assay was performed on genomic DNA isolated from the liver. Asterisk (*) indicates undigested PCR products; black arrows indicate cleavage products. (D) Band intensity of undigested and digested products were measured and analyzed by ImageJ. (E) Two rounds of PCR were performed to amplify junctions between the ROSA26 locus and the human G6Pase transgene from the AAV2/8-RoGP6 vector. Black arrows indicate predicted product size. Group sizes are: AAV, n = 4; AAV+DMSO, n = 3; AAV+BEZ, n = 6; unaffected, n = 4. Mean ± SE is shown. *$p < 0.05$, **$p < 0.01$, ***$p < 0.001$, ****$p < 0.0001$ from ANOVA. BEZ, bezafibrate.

cassettes (66453; Thermo Fisher Scientific/Pierce, Waltham, MA, USA), and were stored at −80°C.

Reagents

Bezafibrate was donated (Roivant Sciences, New York, NY, USA), and DMSO (D8418) was purchased (Sigma Chemical, St. Louis, MO, USA). Protein concentrations were determined with the Pierce BCA assay kit (23225) from Thermo Fisher Scientific (Waltham, MA, USA). Western blotting used Tris/Glycine/SDS Running buffer (161-0732) and polyvinylidene fluoride (PVDF; 162-0177) (Bio-Rad Laboratories, Hercules, CA, USA), ECL substrate reagent (34095; Thermo Fisher Scientific, Waltham, MA, USA), and primary antibodies for PPAR-α (sc398394) and PPAR-γ (sc7273) (Santa Cruz Biotechnology, Dallas, TX, USA), LC3B (2775S; Cell Signaling Technology, Danvers, MA, USA), SIRT1 (07-131; Millipore Sigma, Burlington, MA, USA), and β-actin (A3854; Sigma Chemical, St. Louis, MO, USA). Anti-rabbi or anti-mouse immunoglobulin G (IgG)-conjugated horseradish peroxidase (Santa Cruz) was used as a secondary antibody. The Triglyceride Colormetric Assay Kit (10010303; Cayman Chemical Company, Ann Arbor, MI, USA) was used.

Mouse Experiments

Carrier $G6pc^{+/-}$ mice were bred to produce homozygous $G6pc^{-/-}$ offspring. $G6pc^{-/-}$ mice are phenotypically distinct as neonates and easily distinguishable from their unaffected (+/−) or (+/+) littermates at about 3 days of age, whereupon they are given daily subcutaneous injections of 0.1–0.2 mL 10% dextrose. Bezafibrate was dissolved in a 1:10 DMSO:PBS solution (12.5 mg/kg) and administrated daily through intraperitoneal injection, starting at 5 days of age and continuing for 21 days. The control groups underwent a similar injection schedule with daily intraperitoneal injections of 1:10 DMSO:PBS vehicle or no injections. $G6pc^{-/-}$ mice were injected with vectors via the retro-orbital sinus at 14 ± 1 days of age without regard to sex, and both males and females were included in all groups. Injection was performed following isoflurane anesthesia with a 28G insulin syringe (10 μL/g volume; 1.3×10^{13} vg/kg AAV2/9-RoG6P and 4.8×10^{12} vg/kg AAV2/9-ZFN), and hemostasis was achieved by brief manual pressure. Mice were euthanized for tissue collection at 3 months of age. Tissue from liver and kidney was frozen at −80°C, flash frozen with optimal cutting temperature compound (Tissue-Tek; Sakura Finetek USA, Torrance, CA, USA) for tissue sectioning, and preserved in formalin (VWR, Radnor, PA, USA).

Western Blotting

Liver tissue samples were homogenized in radioimmunoprecipitation assay (RIPA) lysis buffer (Thermo Fisher), and the protein concentration was determined via BCA Assay (Thermo Fisher). Laemmli sample buffer was added (250 mmol/L Tris [pH 7.4], 2% w/v SDS, 25% v/v glycerol, 10% v/v 2-mecaptoethanol, 0.01% w/v bromophenol blue), and gel samples were boiled for 10 min and stored at −20°C until SDS-PAGE was performed. Samples were run on a SDS-polyacrylamide gel and transferred to a polyvinylidene difluoride membrane (Bio-Rad). Washing, blocking, and antibody solutions were prepared in PBS with 0.1% Tween 20 (PBST). Following washing, membranes were blocked for an hour in 5% skim milk, incubated overnight at 4°C with the primary antibodies, washed, and reincubated for an hour with the secondary antibody. After a final wash, enhanced chemiluminescence (ECL) detection reagents (Thermo Fisher) were added

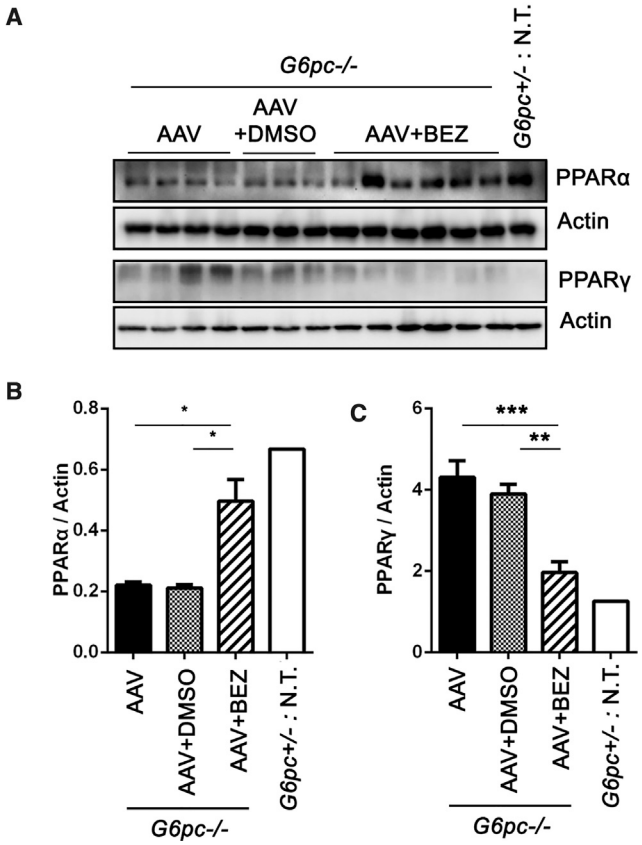

Figure 5. PPAR Signaling in the Liver

(A) Liver cell lysates were prepared and subjected to western blot analysis. (B and C) Band intensity of PPAR-α and -γ (C) was quantified and analyzed by Image-lab software (Bio-Rad) and normalized to *Actin*. Group sizes are: AAV, n = 4; AAV+DMSO, n = 3; AAV+BEZ, n = 6; unaffected, n = 4. Mean ± SE is shown. *p < 0.05, **p < 0.01, ***p < 0.001, ****p < 0.0001 from ANOVA. BEZ, bezafibrate.

to the membrane, and protein signal was read using a ChemiDoc imaging system (Bio-Rad). Membranes were also imaged for β-actin control signal after stripping and re-blocking the membrane.

Biochemical Assays

G6Pase, histochemical staining for G6Pase, and glycogen assays were performed on liver and kidney homogenates using previously described methods.[30] G6Pase was detected qualitatively in frozen sections (6 μm) of mouse liver as described previously.[30] G6Pase-positive cells were counted from 20× fields and analyzed using ImageJ software. *G6pc*$^{-/-}$ mice, 2 weeks of age, were used as a control. Triglyceride concentration in the liver was determined using a colorimetric assay kit (Cayman Chemical) following the manufacturer's instructions.

G6Pase Histochemical Staining

G6Pase was detected qualitatively in frozen sections (6 μm) of mouse liver by using previously described methods.[30,38] G6Pase-positive cells were counted from 10 random different fields of each mouse at ×20 magnification and analyzed using ImageJ software. *G6pc*$^{-/-}$ mice, 2 weeks of age, were used as controls.

GTT

All mice were fasted for 4 h and were given an intraperitoneal injection of 10% dextrose (10 μ/g of body weight). Blood samples were taken at the times indicated from the tail vein of the same animals, and glucose was measured using AlphaTRAK2 Strips (71681-01; Zoetis, Parsippany, NJ, USA) with AlphaTRAK2 Meters.

Real-Time RT-PCR and Quantification of Vector DNA

For quantification of transcripts, total RNA was extracted using Tri Reagent and chloroform extraction method. cDNA was synthesized using a ReverAid First Strand cDNA synthesis Kit (K1622; Thermo Fisher) with random hexamers. Primers used were as follows: hG6PC, 5′-CTGTTCAGCTTCGCCATC-3′, 5′-GGGAGGCTACAA TAGAGCT-3′; PPAR-α, 5′-TCGGCGAACTATTCGGCTG-3′, 5′-G CACTTGTGAAAACGGCAGT-3′; PPAR-γ, 5′-TGTGGGGATAAA GCATCAGGC-3′, 5′- CCGGCAGTTAAGATCACACCTAT-3′; and ACTIN, 5′-AGAGGGAAATCGTGCGTGAC-3′, 5′-CAATAGTGAT GACCTGGCCGT-3′. For quantification of vector DNA, genomic DNA was extracted using Wizard Genomic DNA Purification Kit (A1120; Promega, Fitchburg, WI, USA). Gene-specific primers for the human G6Pase promoter are 5′-CAAAGATCAGGGCTGGG TTGA-3′, 5′-CTTGGTGGTGATTGCTCTGCT-3′.[15] The experiment was performed on LightCycler 480II (Roche, Basel, Switzerland).

Quantification of DNA Repair at the ROSA26 Locus in the Liver (Surveyor Assay)

Liver DNA was extracted using the Wizard Genomic DNA Purification Kit (Promega, Madison, WI, USA). The ROSA26 locus was PCR amplified by Takara ExTaq (Takara Clontech, Mountain View, CA, USA) with the following reagents: 2.5 μL of ExTaq buffer; 2 μL of 2.5 mM dinucleotide triphosphate (dNTP) mix; 1 μL of 10 μM primer SrvF1 (5′-AAGGGAGCTGCAGTGGAGTA-3′);[39] 1 μL of 10 μM primer SrvR1 (5′-GCGGGAGAAATGGATATGAA-3′);[39] 17.3 μL of water, 1 μL (100 ng) of genomic DNA; and 0.2 μL of HotStart ExTaq polymerase. Cycling conditions were: 30 cycles of denaturation at 98°C for 10 s, annealing at 60°C for 10 s, extension at 72°C for 30 s, followed by incubation at 4°C. One microliter of first-round PCR products was used in a nested reaction with the same conditions except primers were SrvFnst (5′-GGGAGGTGTGGGAGGTTT-3′) and SrvRnst (5′-TGGCCACTCGTTTAAACCTC-3′). Second-round PCR products were self-hybridized by incubation in a thermocycler with the following conditions at a −0.1°/s ramp rate: 95°C for 5 min; 85°C for 20 s; 75°C for 20 s; 65°C for 20 s; 55°C for 20 s; 45°C for 20 s; 35°C for 20 s; 25°C for 20 s; followed by incubation at 4°C. Sixteen microliters of the hybridized second-round products were then incubated with 2 μL of 150 mM MgCl2, 1 μL of Surveyor nuclease (706020; IDT), and 1 μL of Surveyor Enhancer S at 42°C for 1 h prior to loading on a 10% PAGE-Tris-borate-EDTA (TBE) gel. The gel was stained with GelRed and analyzed with densitometry to quantify the prevalence of NHEJ DNA repair at the ROSA26 locus.

Urine Organic Acid Quantification

Sodium L-lactate-$^{13}C_3$, sodium pyruvate-$^{13}C_3$, α-ketoglutarate-$^{13}C_4$ (disodium salt), d_3-ethylmalonic acid, d_4-citric acid, sodium D-3-hydroxybutyrate-$^{13}C_4$, 3-methylglutaconic acid (*cis/trans* mix, 2,4-$^{13}C_2$, 3-methyl-^{13}C), and N-methyl-d_3-creatinine were obtained from Cambridge (Cambridge Isotopes Labs, Woburn, MA, USA). Ethyl-d_3-malonic acid was obtained from CDN Isotopes (Pointe-Claire, Quebec, Canada). Unlabeled standards were obtained from Sigma with the exception of N-Isovalerylglycine (Toronto Research Chemicals, Toronto, ON, Canada). Ethoxyamine hydrochloride was purchased from (Thermo Fisher). All other reagents and solvents were purchased from Sigma or VWR.

Urine organic acids were analyzed qualitatively and quantitatively using positive ion electron-impact (EI) gas chromatography-mass spectrometry (GC-MS) on a Trace 1310 gas chromatograph coupled to an ISQ LT mass spectrometer (Thermo Fisher) based upon published methods.[40] For the quantification of the nine selected urine organic acids (lactate, pyruvate, Z- and E-3-hydroxybutyrate, ethylmalonic acid, 3-methylglutaconic acid, isovalerylglycine, alpha-ketoglutarate, citrate), approximately 40–60 μL of mouse urine was diluted with deionized water to 100 μL. A fixed volume (80 μL) of the diluted urine was spiked with 40 μL of a mixture of the isotope-labeled internal standards containing [$^{13}C_3$] sodium L-lactate, [$^{13}C_3$] sodium pyruvate, [$^{13}C_4$]-α-ketoglutarate- (disodium salt), [$^{2}H_3$]-ethylmalonic acid, [$^{2}H_4$]-citric acid, [$^{13}C_4$]-sodium D-3-hydroxybutyrate, and [2,4-$^{13}C_2$, 3-methyl-^{13}C]-3-methylglutaconic acid (*cis/trans* mix) dissolved in deionized water. Samples were basified with sodium bicarbonate and incubated at ambient temperature for 20 min with ethoxyamine hydrochloride to derivatize alpha-ketoacid groups in pyruvate, alpha-ketoglutarate, and similar compounds. Hydrochloric acid (6 mol/L) and an excess of sodium chloride solid were added, and organic acids were repeatedly extracted four times using liquid-liquid extraction with ethyl acetate. The four ethyl acetate extracts were combined and dried under a nitrogen stream. Pyridine, tetracosane (as an external standard), and N,O-bis(trimethylsilyl) trifluoroacetamide (BSTFA) were added to the dried extracts. Samples were derivatized at 90°C for 20 min, transferred to injection vials, and 1 μL was injected into the GC-MS with a 1:10 split ratio. Analytes were separated on a 100% dimethylpolysiloxane column (0.25 mm × 30 m, 1.0-μm film thickness, RXi-1ms; Restek Corporation, Bellefonte, PA, USA) with a temperature gradient of 8°C/min from 120°C to 300°C. Analytes were detected by full-scan analysis from mass/Z (m/z) 50–550 with a 0.2-s scan time. Analyte concentrations were calculated by extrapolation from six-point calibration curves, which were constructed by plotting the response (extracted ion area ratios for analytes and internal standards) against calibrator concentration. Details of the ion ratios and calibrator concentrations used are shown (Table S2). Qualitative analysis was performed by identification of sample components from their EI mass spectra and retention times, based on comparison with a customized and a commercial mass spectral library (NIST Mass Spectral Library v14). For creatinine analysis, a 10-μL aliquot of the diluted urine was combined with 10 μL of 3.2 mmol/L d3-creatinine and analyzed using stable isotope dilution electrospray-tandem mass spectrometry (ESI-MS/MS) as previously described.[41] The concentrations of organic acids relative to the creatinine concentration were calculated and compared between groups.

Statistics

Statistical analysis was performed using GraphPad Prism 6. Statistical significance was determined by one-way ANOVA with Tukey's multiple comparisons test. The statistical significance of comparisons is indicated as *$p < 0.05$, **$p < 0.01$, ***$p < 0.001$, and ****$p < 0.0001$.

SUPPLEMENTAL INFORMATION

Supplemental Information includes two tables and two figures and can be found with this article online at https://doi.org/10.1016/j.omtm.2019.02.002.

AUTHOR CONTRIBUTIONS

Conceptualization, H.R.K. and D.D.K.; Methodology, H.R.K. and D.D.K.; Investigation, H.R.K., L.R.W., A.M.S., D.J.L., and S.P.Y.; Manuscript Writing, H.R.K. and D.D.K.; Review & Editing, H.R.K. and D.D.K.; Funding Acquisition, D.D.K. and H.R.K.

CONFLICTS OF INTEREST

D.D.K. served on a data and safety monitoring board for Baxter International. He was supported by a grant from Enzavant. He received an honorarium and grant support in the past from Genzyme Sanofi. He holds equity in Actus Therapeutics. He has developed the technology that is being used in the study. If the technology is commercially successful in the future, the developers and Duke University may benefit financially.

ACKNOWLEDGMENTS

The authors also would like to acknowledge technical support from Songtao Li for mouse breeding and from Steve Hillman for urine organic acid analysis. The authors would also like to acknowledge inspiration and support from Dr. Emory and Mary Chapman and their son Christopher, and from Dr. John and Michelle Kelly. We deeply appreciate the dedication shown by the staff of the Duke Department of Laboratory Animal Resources, as well as undergraduate students at Duke University. We thank Dr. Janice Chou at the National Institute of Child Health and Human Development for providing *G6pc*$^{-/-}$ mice. This work was supported by grant R01DK105434-03 from the National Institute of Diabetes and Digestive and Kidney Diseases, and by the resources of the Alice and Y. T. Chen Center for Genetics and Genomics. H.-R.K. was funded by a Pfizer NC Biotechnology Gene Therapy Fellowship (Agreement GTF-A-4026).

REFERENCES

1. Chou, J.Y., Jun, H.S., and Mansfield, B.C. (2010). Glycogen storage disease type I and G6Pase-β deficiency: etiology and therapy. Nat. Rev. Endocrinol. *6*, 676–688.

2. Koeberl, D.D., Kishnani, P.S., Bali, D., and Chen, Y.T. (2009). Emerging therapies for glycogen storage disease type I. Trends Endocrinol. Metab. *20*, 252–258.

3. Chen, Y.T., Bazzarre, C.H., Lee, M.M., Sidbury, J.B., and Coleman, R.A. (1993). Type I glycogen storage disease: nine years of management with cornstarch. Eur. J. Pediatr. *152* (*Suppl 1*), S56–S59.

4. Kishnani, P.S., Austin, S.L., Abdenur, J.E., Arn, P., Bali, D.S., Boney, A., Chung, W.K., Dagli, A.I., Dale, D., Koeberl, D., et al.; American College of Medical Genetics and Genomics (2014). Diagnosis and management of glycogen storage disease type I: a practice guideline of the American College of Medical Genetics and Genomics. Genet. Med. *16*, e1.

5. Wolfsdorf, J.I., Rudlin, C.R., and Crigler, J.F., Jr. (1990). Physical growth and development of children with type 1 glycogen-storage disease: comparison of the effects of long-term use of dextrose and uncooked cornstarch. Am. J. Clin. Nutr. *52*, 1051–1057.

6. Koeberl, D.D., Kishnani, P.S., and Chen, Y.T. (2007). Glycogen storage disease types I and II: treatment updates. J. Inherit. Metab. Dis. *30*, 159–164.

7. Keeler, A.M., ElMallah, M.K., and Flotte, T.R. (2017). Gene therapy 2017: progress and future directions. Clin. Transl. Sci. *10*, 242–248.

8. Halbert, C.L., Standaert, T.A., Aitken, M.L., Alexander, I.E., Russell, D.W., and Miller, A.D. (1997). Transduction by adeno-associated virus vectors in the rabbit airway: efficiency, persistence, and readministration. J. Virol. *71*, 5932–5941.

9. Halbert, C.L., Rutledge, E.A., Allen, J.M., Russell, D.W., and Miller, A.D. (2000). Repeat transduction in the mouse lung by using adeno-associated virus vectors with different serotypes. J. Virol. *74*, 1524–1532.

10. Demaster, A., Luo, X., Curtis, S., Williams, K.D., Landau, D.J., Drake, E.J., Kozink, D.M., Bird, A., Crane, B., Sun, F., et al. (2012). Long-term efficacy following readministration of an adeno-associated virus vector in dogs with glycogen storage disease type Ia. Hum. Gene Ther. *23*, 407–418.

11. Weinstein, D.A., Correia, C.E., Conlon, T., Specht, A., Verstegen, J., Onclin-Verstegen, K., Campbell-Thompson, M., Dhaliwal, G., Mirian, L., Cossette, H., et al. (2010). Adeno-associated virus-mediated correction of a canine model of glycogen storage disease type Ia. Hum. Gene Ther. *21*, 903–910.

12. Koeberl, D.D., Sun, B.D., Damodaran, T.V., Brown, T., Millington, D.S., Benjamin, D.K., Jr., Bird, A., Schneider, A., Hillman, S., Jackson, M., et al. (2006). Early, sustained efficacy of adeno-associated virus vector-mediated gene therapy in glycogen storage disease type Ia. Gene Ther. *13*, 1281–1289.

13. Cunningham, S.C., Dane, A.P., Spinoulas, A., Logan, G.J., and Alexander, I.E. (2008). Gene delivery to the juvenile mouse liver using AAV2/8 vectors. Mol. Ther. *16*, 1081–1088.

14. Yiu, W.H., Lee, Y.M., Peng, W.T., Pan, C.J., Mead, P.A., Mansfield, B.C., and Chou, J.Y. (2010). Complete normalization of hepatic G6PC deficiency in murine glycogen storage disease type Ia using gene therapy. Mol. Ther. *18*, 1076–1084.

15. Landau, D.J., Brooks, E.D., Perez-Pinera, P., Amarasekara, H., Mefferd, A., Li, S., Bird, A., Gersbach, C.A., and Koeberl, D.D. (2016). In vivo zinc finger nuclease-mediated targeted integration of a glucose-6-phosphatase transgene promotes survival in mice with glycogen storage disease type IA. Mol. Ther. *24*, 697–706.

16. Sun, B., Li, S., Yang, L., Damodaran, T., Desai, D., Diehl, A.M., Alzate, O., and Koeberl, D.D. (2009). Activation of glycolysis and apoptosis in glycogen storage disease type Ia. Mol. Genet. Metab. *97*, 267–271.

17. Kim, S.Y., and Bae, Y.S. (2009). Cell death and stress signaling in glycogen storage disease type I. Mol. Cells *28*, 139–148.

18. Dikic, I., and Elazar, Z. (2018). Mechanism and medical implications of mammalian autophagy. Nat. Rev. Mol. Cell Biol. *19*, 349–364.

19. Ezaki, J., Matsumoto, N., Takeda-Ezaki, M., Komatsu, M., Takahashi, K., Hiraoka, Y., Taka, H., Fujimura, T., Takehana, K., Yoshida, M., et al. (2011). Liver autophagy contributes to the maintenance of blood glucose and amino acid levels. Autophagy *7*, 727–736.

20. Hösel, M., Huber, A., Bohlen, S., Lucifora, J., Ronzitti, G., Puzzo, F., Boisgerault, F., Hacker, U.T., Kwanten, W.J., Klöting, N., et al. (2017). Autophagy determines efficiency of liver-directed gene therapy with adeno-associated viral vectors. Hepatology *66*, 252–265.

21. Willson, T.M., Brown, P.J., Sternbach, D.D., and Henke, B.R. (2000). The PPARs: from orphan receptors to drug discovery. J. Med. Chem. *43*, 527–550.

22. Wang, Y.X. (2010). PPARs: diverse regulators in energy metabolism and metabolic diseases. Cell Res. *20*, 124–137.

23. Cho, J.H., Kim, G.Y., Pan, C.J., Anduaga, J., Choi, E.J., Mansfield, B.C., and Chou, J.Y. (2017). Downregulation of SIRT1 signaling underlies hepatic autophagy impairment in glycogen storage disease type Ia. PLoS Genet. *13*, e1006819.

24. Lee, J.M., Wagner, M., Xiao, R., Kim, K.H., Feng, D., Lazar, M.A., and Moore, D.D. (2014). Nutrient-sensing nuclear receptors coordinate autophagy. Nature *516*, 112–115.

25. Lee, J.M. (2016). Transcriptional coordination of hepatic autophagy by nutrient-sensing nuclear receptor PPARα and FXR. Ann. Pediatr. Endocrinol. Metab. *21*, 193–198.

26. Farah, B.L., Landau, D.J., Sinha, R.A., Brooks, E.D., Wu, Y., Fung, S.Y.S., Tanaka, T., Hirayama, M., Bay, B.H., Koeberl, D.D., and Yen, P.M. (2016). Induction of autophagy improves hepatic lipid metabolism in glucose-6-phosphatase deficiency. J. Hepatol. *64*, 370–379.

27. Waskowicz, L.R., Zhou, J., Landau, D.J., Brooks, E.D., Lim, A., Yavarow, Z.A., Kudo, T., Zhang, H., Wu, Y., Grant, S., et al. (2019). Bezafibrate induces autophagy and improves hepatic lipid metabolism in glycogen storage disease type Ia. Hum. Mol. Genet. *28*, 143–154.

28. Koeberl, D.D., Pinto, C., Sun, B., Li, S., Kozink, D.M., Benjamin, D.K., Jr., Demaster, A.K., Kruse, M.A., Vaughn, V., Hillman, S., et al. (2008). AAV vector-mediated reversal of hypoglycemia in canine and murine glycogen storage disease type Ia. Mol. Ther. *16*, 665–672.

29. Lei, K.J., Chen, H., Pan, C.J., Ward, J.M., Mosinger, B., Jr., Lee, E.J., Westphal, H., Mansfield, B.C., and Chou, J.Y. (1996). Glucose-6-phosphatase dependent substrate transport in the glycogen storage disease type-1a mouse. Nat. Genet. *13*, 203–209.

30. Luo, X., Hall, G., Li, S., Bird, A., Lavin, P.J., Winn, M.P., Kemper, A.R., Brown, T.T., and Koeberl, D.D. (2011). Hepatorenal correction in murine glycogen storage disease type I with a double-stranded adeno-associated virus vector. Mol. Ther. *19*, 1961–1970.

31. Weinstein, D.A., Somers, M.J., and Wolfsdorf, J.I. (2001). Decreased urinary citrate excretion in type 1a glycogen storage disease. J. Pediatr. *138*, 378–382.

32. Li, S., Sun, B., Nilsson, M.I., Bird, A., Tarnopolsky, M.A., Thurberg, B.L., Bali, D., and Koeberl, D.D. (2013). Adjunctive β2-agonists reverse neuromuscular involvement in murine Pompe disease. FASEB J. *27*, 34–44.

33. Han, S.O., Li, S., Bird, A., and Koeberl, D. (2015). Synergistic efficacy from gene therapy with coreceptor blockade and a β2-agonist in murine Pompe disease. Hum. Gene Ther. *26*, 743–750.

34. Ronzitti, G., and Mingozzi, F. (2018). Combination therapy is the new gene therapy? Mol. Ther. *26*, 12–14.

35. Li, H., Haurigot, V., Doyon, Y., Li, T., Wong, S.Y., Bhagwat, A.S., Malani, N., Anguela, X.M., Sharma, R., Ivanciu, L., et al. (2011). In vivo genome editing restores haemostasis in a mouse model of haemophilia. Nature *475*, 217–221.

36. Ghosh, A., Allamarvdasht, M., Pan, C.J., Sun, M.S., Mansfield, B.C., Byrne, B.J., and Chou, J.Y. (2006). Long-term correction of murine glycogen storage disease type Ia by recombinant adeno-associated virus-1-mediated gene transfer. Gene Ther. *13*, 321–329.

37. Lee, Y.M., Jun, H.S., Pan, C.J., Lin, S.R., Wilson, L.H., Mansfield, B.C., and Chou, J.Y. (2012). Prevention of hepatocellular adenoma and correction of metabolic abnormalities in murine glycogen storage disease type Ia by gene therapy. Hepatology *56*, 1719–1729.

38. Jonges, G.N., Van Noorden, C.J., and Gossrau, R. (1990). Quantitative histochemical analysis of glucose-6-phosphatase activity in rat liver using an optimized cerium-diaminobenzidine method. J. Histochem. Cytochem. *38*, 1413–1419.

39. Perez-Pinera, P., Ousterout, D.G., Brown, M.T., and Gersbach, C.A. (2012). Gene targeting to the ROSA26 locus directed by engineered zinc finger nucleases. Nucleic Acids Res. *40*, 3741–3752.

40. Sweetman, L. (1991). "Organic Acid Analysis" in Techniques in Diagnostic Human Biochemical Genetics: A Laboratory Manual (Wiley-Liss), pp. 143–176.

41. Young, S.P., Zhang, H., Corzo, D., Thurberg, B.L., Bali, D., Kishnani, P.S., and Millington, D.S. (2009). Long-term monitoring of patients with infantile-onset Pompe disease on enzyme replacement therapy using a urinary glucose tetrasaccharide biomarker. Genet. Med. *11*, 536–541.